

RSC Advances



This is an *Accepted Manuscript*, which has been through the Royal Society of Chemistry peer review process and has been accepted for publication.

Accepted Manuscripts are published online shortly after acceptance, before technical editing, formatting and proof reading. Using this free service, authors can make their results available to the community, in citable form, before we publish the edited article. This *Accepted Manuscript* will be replaced by the edited, formatted and paginated article as soon as this is available.

You can find more information about *Accepted Manuscripts* in the [Information for Authors](#).

Please note that technical editing may introduce minor changes to the text and/or graphics, which may alter content. The journal's standard [Terms & Conditions](#) and the [Ethical guidelines](#) still apply. In no event shall the Royal Society of Chemistry be held responsible for any errors or omissions in this *Accepted Manuscript* or any consequences arising from the use of any information it contains.

Mesenchymal stem cells (MSC) viability on PVA and PCL polymers coated hydroxyapatite scaffolds derived from cuttlefish

S.A. Siddiqi¹, F. Manzoor¹, A. Jamal¹, M. Tariq², R. Ahmad³, M. Kamran⁴, A. Chaudhry¹, I.U. Rehman^{1,5}

1-Interdisciplinary Research Centre in Biomedical Materials (IRCBM), COMSATS Institute of Information Technology Defence Road, Off Raiwind Road, Lahore 54600 Pakistan

2-Department of Biology, Syed Babar Ali School of Science and Engineering, Lahore University of Management Sciences, DHA, Lahore Pakistan

3- Department of Physics, G.C. University, Kutchery Road, Lahore-54500, Pakistan

4- College of Engineering and Emerging Technologies, University of the Punjab, Lahore-54590, Pakistan

5-Department of Material Science and Engineering, The Kroto Research Institute, University of Sheffield, Broad Lane, S3 7HQ, Sheffield, UK

Abstract

In the present study, cuttlefish bones are used to prepare highly porous hydroxyapatite (HA) scaffolds via hydrothermal treatment at 200°C. Raw cuttlefish bones (CB) and the hydrothermal products have been analyzed and compared for their composition and microstructure using X-ray powder diffraction (XRD), Optical Microscopy (OM), Scanning Electron Microscopy (SEM), Fourier Transform Infrared Spectroscopy (FTIR), porosity estimation and compressive strength measuring techniques. Characterization reveals that cuttlebone has high porosity approaching above 70%, possesses the laminar structure of aragonite mixed with some organic materials. The compressive strength of the CB-HA is improved after coating with both polyvinyl alcohol (PVA) and polycaprolactone (PCL). Furthermore, our in vitro biocompatibility studies revealed that CB-HA and PVA coated CB-HA scaffolds are non-cytotoxic and supported the adherence and proliferation of rMSC i.e., comparable to pure HA scaffolds. Altogether, our results suggest that naturally derived CB-

HA, PVA and PCL coated CB-HA scaffolds, are potential cheap candidates for bone tissue engineering applications and also that PVA and PCL coating on them provides better mechanical strength.

Keywords: Cuttlefish bone scaffolds, Hydroxyapatite scaffolds, Mesenchymal cell viability, polymer coatings on scaffolds, In vitro SBF studies

1 Introduction

Bone abnormalities, trauma and aesthetic procedures rely on using biologically derived and/or synthetic bone grafts. The tissue regeneration strategy however is also gaining attention along with tissue replacement approach in last couple of decade¹. The development of porous scaffolds for tissue regeneration application is of prime interest. The scaffolds materials used for bone tissue engineering (BTE) should have resemblance with both structural and mechanical properties of natural bone. In addition, porous scaffolds used in tissue engineering facilitate cell attachment, proliferation, differentiation and blood vessel formation that eventually lead to specific tissue development^{2, 3}. Beside porosity other important features of scaffolds include biodegradability and certain level of mechanical strength to hold out against certain level of physiological loading. Bone is primarily composed of calcium phosphate, mainly hydroxyapatite (HA) $[\text{Ca}_{10}(\text{PO}_4)_6(\text{OH})_2]$ and collagen. HA which is also known as artificial bone material has tremendous resemblance with mineral phase of natural bone⁴. During last decade porous bio-ceramics has taken a lot of attention due to their indifferent properties such as vascularization, bone cell invasion and angiogenesis⁵. Synthetic materials are helping surgeons to meet the need of biomaterials in

BTE⁶. Lately natural materials however have been used to achieve the required properties for bone regeneration and tissue engineering applications, biomaterials derived from several natural sources such as corals⁶, seashells⁷, animal bones⁸ cuttlefish bone⁹ have been implied in bone tissue engineering field. In 1974, corals were converted into hydroxyapatite by hydrothermal method firstly by Roy and Linnehan¹⁰. They found complete conversion of aragonite using phosphates into hydroxyapatite at 270°C and at 103 MPa. Sivakumar et al. reported hydroxyapatite derivation from Indian corals via hydrothermal process¹¹. Hydroxyapatite scaffolds, first of all were synthesized by hydrothermal transformation of cuttlefish bone in 2005¹² and later on were shown to exhibit good biocompatibility^{13, 14}. These previous studies suggest that hydrothermally converted cuttlefish bone into HA can be used as a bone scaffold in tissue engineering. However due to its brittle nature and low mechanical strength limits its application in bone tissue engineering. Thus to enhance the compressive strength and mechanical integrity of scaffolds coating is performed with different biodegradable polymers¹⁵ like poly (lactic-co-glycolic acid) (PLGA), polycaprolactone (PCL) and polyvinyl alcohol (PVA). PCL is very useful for this purpose; it improves the compressive strength of porous scaffolds¹⁶ since its fracture energy is quite higher as compared with other polymers¹⁷. PVA due to its semi permeable nature allows the easy accessibility of nutrients and oxygen to cells and also facilitate the removal of wastes secreted by cells. Moreover because of the controllable degradation, excellent chemical stability (long term temperature and pH stability) and flexibility PVA has been implicated in developing porous bone TE scaffold.

The aim of our work is to enhance and also to compare the compressive strengths of cuttlefish bone transformed HA scaffolds by coating with PCL and PVA. We fabricated HA porous scaffolds by

hydrothermal reaction and subsequently coated them with PCL and PVA. The morphological changes, mechanical properties and biocompatibility of these coated and uncoated scaffolds were examined with rat bone marrow derived MSC in vitro.

2 Materials and methods:

Cuttlefish bones were purchased from the local grocery market. The supply comes from Karachi, Pakistan, where vendors collect cuttlefish bones from seashores. Cuttlefish belongs to Sepiida family and is abundantly found throughout the world's ocean waters. Locally this marine product is known as "Sumandary Jhaag" and used as supplementary animal diet for calcium deficiency especially for parrots. The cuttlefish bones were cleaned and thoroughly washed with distilled water and then dried in a drying oven at 80°C for 24 h. All chemicals used in this study were of analytical grade (di-ammonium hydrogen phosphate, $(\text{NH}_4)_2\text{HPO}_4$, AppliChem BioChemica, Polycaprolactone, PCL, Sigma Aldrich $M_w=70,000$). Commercial hydroxyapatite powder (Plasma Biotol, sintered grade) was used in cell attachment and viability studies.

2.1 Conversion of Cuttlefish Bone into Hydroxyapatite

CB is converted into hydroxyapatite by using hydrothermal treatment according to a reported method¹⁸. Pre-cleaned and dried CB was cut into small pieces and heated at 350°C for 3 h to burn away any organic material present. Then di-ammonium hydrogen phosphate solution was added as phosphorus (P) source with CB which was a calcium (Ca) source in the Teflon vessel by keeping Ca/P = 1.67. It was tightly closed in the steel vessel and placed at 200°C for 6h in the oven. Afterwards they were washed with boiling water and dried at 80°C for 24 h in a vacuum oven.

2.2 PCL/PVA coating of Scaffolds

Polycaprolactone (PCL) was coated on the scaffolds by a reported procedure¹⁹. PCL pellets were dissolved in chloroform at concentrations of 5 % (w/v). Pre-prepared CB-HA scaffolds (1x1x1 cm³) were dipped into the PCL solution under vacuum for 15 min to allow for complete infiltration into the porous scaffold structure. The coated samples were removed from PCL solution and excess solution was removed by placing coated samples on a Whatman filter paper, dried in an oven for 6 h at 40°C, and then let them get dried again for 7 days at room temperature to evaporate residual organic solvent.

A similar procedure was adopted for PVA coating on the scaffolds using de-ionized water at 80°C. The samples were sealed in polythene zipper bags for storage and further analysis.

2.3 In Vitro studies in Simulated Body Fluid (SBF)

The SBF solution was prepared according to the method proposed by Kokubo²⁰. The PCL coated scaffolds and raw CB scaffolds were immersed in SBF solution at 37°C for 14 days and the solution was exchanged each 3rd day during the experiments. After the immersion period was terminated, the samples were removed from the incubator, rinsed gently with deionized water and with 70% ethanol, in sequence. The samples were left to dry at 50°C for 2h and then for 7 days at room temperature in order to obtain stability. Finally, all the samples were analyzed by FTIR and SEM for evaluation of chemical composition and morphology of newly formed bioactive minerals on the surface of the samples.

2.4 X-ray Diffraction (XRD) Study

The crystalline phase identification of the CB, HA-CB, HA-PVA and HA-PCL samples was done by X-ray Powder Diffraction (XRD) analysis technique using MPD XP'ERT PRO Diffractometer (PAN Analytical, The Netherlands) with monochromatic Cu-K α X-radiation, $\lambda = 0.15418$ nm. The scans were taken in 2θ range $\sim 20^\circ$ - 80° with a step size at 0.02° after every 1s. Identification was performed by comparing the experimental XRD patterns to the standards compiled by the Joint Committee on Powder Diffraction Standards (JCPDS) using the cards 00-001-0628 for aragonite and 09-0432 for HA.

2.5 Scanning Electron Microscopy (SEM)

The morphology and pore structure of scaffolds were studied using scanning electron microscope (SEM), JSM-6480 of JOEL, Japan. The samples were mounted with conducting silver paste and sputter coated with gold in order to avoid charging effect on the surface due to electron beam. SEM images were collected in the secondary electron image (SEI) mode.

2.6 Fourier-Transform Infrared Spectroscopy (FTIR)

Structural characterization and functional groups identification was performed using Fourier Transform Infrared Spectroscopy (FT-IR), Thermo Nicolet 6700, USA, with photo-acoustic mode. Total of 256 scans were performed with wave-number range 4000cm^{-1} to 400cm^{-1} with 8cm^{-1} spectral resolution.

2.7 Compression Testing

Compressive strength of samples was studied with the help of Universal Testing Machine (UTM Testometric M500-50AT, United Kingdom). The dimensions of samples were 2 cm³ and they were uniaxially loaded with the cross head speed of 1.0 mm/minute. Five number of samples were used for each test.

2.8 Porosity Test

The porosity (P) of the scaffolds was calculated by the liquid displacement method²¹. Briefly, dried samples were dipped into the known volume (V₁) of dehydrated alcohol to saturate it for 48 h. Noted the volume of alcohol after immersing the scaffold (V₂) and V₃ is the volume after taking out the scaffold from alcohol. Hence V₂-V₃ is the volume of scaffold. The porosity (P) was calculated by using formula:

$$\%P = \frac{V_1 - V_3}{V_2 - V_3} \times 100$$

2.9 In vitro culture of rat mesenchymal stem cells (rMSC)

Rat Mesenchymal Stem Cells (rMSC) were isolated from femur of 4-5 weeks rats using direct adherence method²². The femur was isolated under sterile conditions. A disposable aseptic syringe was used to draw antibiotic supplemented L-DMEM medium repeatedly in and out of bone marrow cavity and the cells fraction was collected in a sterile petri dish. The obtained cell suspension was centrifuged at 250xg for 5 minutes. The cell pellet was re-suspended in DMEM (Gibco) containing 10% FBS (Gibco) and 0.1% penicillin and streptomycin (Gibco) and transferred to T25 tissue culture

flask. The flasks were incubated at 37 °C in a 5 % CO₂ incubator. Cells isolated from one rat were cultured in a flask. The first medium was changed after 4 days. Later on the medium was changed on alternative days until the cells become 70 – 80 % confluent. MSC were sub-cultured at 70 – 80 % confluence. The cells were trypsinized, counted (dead cells excluded by trypan blue assay) and passaged in T-75 flasks. Second- or third-passage MSC were used for cytotoxicity and SEM analysis. All the cell culture experiments performed in this study followed the Biosafety and Ethical Rules and Regulations governed by the Ethical Committee of Animal Handling for Experimentation, University of Veterinary and Animal Sciences, Lahore. The present study was limited on rats and no human trials or experiments were performed.

2.10 Cytotoxicity Assay

Cellular toxicity was determined by 3-(4,5-Dimethylthiazol-2-yl)-2,5-diphenyltetrasodium bromide (MTT) assay^{22, 23}. Prior to cell culture, all the scaffolds included in this study, a) pure HA, b) cuttlefish bone derived HA and c) cuttlefish bone derived HA coated with PVA scaffolds, were sterilized under UV light for 6 hrs/autoclave. Immediately before cell seeding the scaffolds were washed 2-3 times with PBS and pre-conditioned in DMEM medium for an hour. MSC were seeded in 24-well cell culture plate with 5×10^4 cells per well with or without scaffolds. Cells seeded in 24-plate wells without scaffold were used as positive control. Culture plate containing scaffolds but no rMSCs was used as negative control. Post day 7 the medium was discarded and cells/scaffolds were washed with 1 ml PBS. 1 ml (0.5 mg/ml) MTT solution was added to each well and the plate was incubated at 37°C for 3 hrs. The MTT solution was discarded and the cells/scaffolds were washed once with 1 ml PBS. To solubilize the formazan crystals 0.5 ml dimethyl sulfoxide (DMSO) was added to each well and the plate was kept under shaking for 15-20 minutes. The optical density (OD) of the dissolved crystals was measured by using microplate reader at 590 nm. The assay was set up in triplicate with MSC derived from 3 different rats for each sample. % Viability is represented as mean \pm SD of 3

independent experiments. A standard approach for determination of % Viability of cells was adopted in this study²⁴. % Viability of calculated using the following formula:

$$\% \text{ Viability} = \frac{\text{Absorbance (sample)} - \text{Absorbance (Blank)}}{\text{Absorbance (control)} - \text{Absorbance (Blank)}} \times 100$$

2.11 Cell Attachment

To examine the cell attachment capacity on to the scaffolds, 10^5 rMSC were loaded on each scaffold for an hour and cultured in 1 ml medium. After day 5 the medium was discarded. The cells/scaffolds were washed once with 1 ml PBS. The cells were fixed in 4% paraformaldehyde (PFA) for 30 minutes at 37°C and rinsed with 1 ml distil water. The scaffolds were air dried at room temperature overnight. The cells attachment on the scaffolds was observed using scanning electron microscopy (SEM)

3 Results and Discussion

3.1 X-ray Diffraction analysis

The XRD patterns of raw CB and HA-CB are shown in the Figure 1. The patterns were identified by standard Joint Committee on Powder Diffraction Standards, JCPDS file. The diffraction peaks of CB in Fig. 1 (b) matched very well with that of standard aragonite, CaCO_3 , pattern ICDD 00-001-0628. Whereas the pattern for the hydrothermally converted CB, as given in Fig. 1(b), is completely different and gave a good match to pattern ICDD 00-009-0432 of synthetic HA¹⁸. The Miller indices (0

0 2), (2 1 1), (1 1 2), (3 0 0), (1 3 0) and (2 2 2) related to hydroxyapatite are shown in the Fig. 1 (a) ²⁵. Similar conversion of CB into hydroxyapatite has also been reported before by Kim et al and some other authors as well ^{18, 19}. The conversion of aragonite into HA by hydrothermal method (HT) at 200°C has been reported to achieve in one hour by the previous authors. However, the HT product may not be consisting of pure HA. Rocha et al ²⁶ indicated that after 9 h of HT complete conversion of aragonite into HA takes place. We have also carried out similar study and have found out that 6 h are sufficient to get full conversion into single phase HA as depicted by Fig 1.

3.2 FT-IR Spectroscopy

FT-IR spectra of CB and HA-CB samples are shown in the Fig. 2 (a, g) respectively. The spectra show changes in the Infrared (IR) active CO_3^{2-} , OH^- , and PO_4^{3-} bands of CB (aragonite) and HA-CB. The IR active CO_3^{2-} peaks are revealed in the spectrum of CB at 1460-1520 (ν_3), 1088 (ν_1), 852 (ν_2) and doublet peak at 712, 710 (ν_4) cm^{-1} . After HT treatment at 200°C, Fig. 2(b), the conversion of CB into HA is evident by the appearance of PO_4^{3-} tetrahedral whose fundamental vibrational modes appear at 1024 -1086 cm^{-1} (ν_3), a small shoulder peak at 960 (ν_1) and 560, 604 (ν_4) cm^{-1} . Stretching and bending modes of OH^- can be observed at 3250-3575 cm^{-1} and 633 cm^{-1} respectively. However, in the FT-IR spectrum for HA-CB, Fig. 2 (b), this OH^- mode is not very prominent. Our XRD results further verify the conversion from aragonite to HA, as can be seen in Fig. 2 (b). Ivankokovic et al ⁹ have also observed a similar trend, weakness or absence, of this stretching mode and has indicated that it is due to lack of crystallinity in the material. Furthermore, the HA-CB was coated with PVA and PCL, subsequently, the FT-IR spectra for these samples also show similar trend of weaker OH^- mode at 3250-3575 cm^{-1} . The FT-IR spectra for PVA and PCL coated HA-CB and CB are shown in Fig. 2 (c), (d), (g), respectively. In these spectra the peak at 3000 cm^{-1} is due to the stretching band of C-H while peak at 1740 cm^{-1} is due to the -C=O of PCL. In Fig 2 (c) and (g) the broader peaks of OH is due to the coating of PVA on HA-CB

and CB respectively. Table 1, provides a summary of the various modes observed in these FT-IR spectra for a quick analysis.

Peak (cm ⁻¹)	Description	Reference Fig.	References
555	Triply degenerated bending mode(ν_4) of the O-P-O bonds of the phosphate group	B, C, D, E	27, 28
605	Triply degenerated bending mode(ν_4) of the O-P-O bonds of the phosphate group	B, C, D, E	15, 27, 28
852, 1790	Stretching mode (ν_3) of the CO ₃ ²⁻ group in HA	A, B, C, D, E, F, G	29
1088	Triply degenerated asymmetric stretching mode, ν_3 , of the P-O bond of the phosphate group	A, B, C, D, E, F, G	27, 28
1460	Bending mode (ν_4 or ν_3) of the CO ₃ ²⁻ group in A and B-type Hap	A, B, C, D, E, F, G	30
1480-1520	Characteristic stretching mode (ν_3) of the CO ₃ ²⁻ group in Hap	A, B, C, D, E, F, G	29, 30
633	Vibrational mode ν_1 of the hydroxyl group	B, C, D, E, F	29
3482	Stretching mode (ν_1) of the hydroxyl group	A, B, C, D, F, G	29
2850-2960	Stretching mode of -C-H in due to PCL	D, F	31, 32
1740	Due to -C=O of PCL	D, F	31, 32

Table 1: FTIR spectroscopy data for various modes observed in the Fig. 2

3.3 Scanning Electron Microscopy Analysis

Fig. 3 shows SEM images of raw CB, HA-CB, PVA and PCL coated CB. These micrographs show that the CB microstructure, in all cases, is highly porous and the pores, rectangular in shape, are large and interconnected. Furthermore the micrographs demonstrate that the hydrothermal conversion process does not alter much the natural interconnected porous structures of CB. SEM micrographs show the internal structure of bone in which lamellae are separated by pillars. The pillars have height in the range of 70-100 μm and separation of pillars is 30-70 μm which varied from position to position. The thin layer of PCL coated on CB, as shown in Fig 3c, appeared to be uniformly covering the entire structure. It is also evident that the large pores are not filled, they remain opened. One of the most important requirements for hosting physiological activities such as vascularization and tissue growth is the presence of interconnected right sized large and small pores³³ as can be seen in the SEM micrographs, Fig 3, of all type of the CB samples whether coated with polymer or uncoated.

In vitro SBF study on both type of scaffolds, CB without PCL coating and HA-CB with PCL coating, was carried out to see the effect of polymer coating. The results are shown in SEM images in Figs 3 d,e, respectively. It is evident that non-coated scaffold, Fig 3d, is structurally degraded when exposed to SBF solution. On the other hand the pillar like structure of CB-HA remains fully in contact and the formation of an apatite layer can clearly be seen on the PCL coated scaffold, as shown in Fig. 3e. The formation of the apatite layer has slightly reduced the pore size, also verified by the porosity measurements. The SEM analysis indicates that PCL coating provides the outstanding stability to the structure. Similar observation of structural stability and apatite layer formation on the scaffolds after SBF study were also observed for PVA coated samples (provided in supplementary S.Fig.1).

3.4 Compressive strength

The compressive strengths are measured for two sets of samples. One set consists of CB and PVA coated CB. The second set consists of three samples, uncoated CB-HA, PVA and PCL coated CB-HA. The derived compressive strengths are shown in Fig. 4. According to the SEM images as shown in Fig 3, CB microstructure consists of parallel pillars repeating themselves at almost regular intervals. In one direction this gap is from 30-70 μm and in its perpendicular direction it is from 70-100 μm . The literature review suggests that these pillars in CB are of aragonite¹⁶. During the process of data acquisition for stress-strain curves, systematic fluctuations were observed. They are due to systematically breakage of pillars of aragonite followed by a relatively large flat area of porous tetragon in the scaffold, inconsistent with their SEM images in Fig 3. As the CB microstructure is highly ordered, due to parallel array of pillars, the measurement of compressive strength becomes direction dependent. In our case we have tried to hold the scaffold samples clamped perpendicular the heights of the pillars.

UTM analysis results are shown in Fig 4. The compressive strength of the water washed raw CB is 0.609 MPa that decreases to 0.376 MPa for CB-HA scaffolds. It is interesting to note that the original pillar like microstructure, as shown in Fig 3, is preserved even after its HT conversion to HA. The decrease in compressive strength is obvious. This is due to burning of organic materials present inside that provides mechanical support to the whole structure. But when heated at 350°C followed by the heating in hydrothermal (high pressure) at 200°C for 4 h the resultant material lose strength. However, the compressive strengths of both the raw CB and CB-HA are convincingly increased after their coating with PVA and PCL polymers. The compressive strength value of for PVA coated CB increased almost 100% to 1.275 MPa. The decrease in strength can be improved by coating the scaffolds with polymers like PCL and PVA. When CB-HA scaffolds are coated with PCL its compressive strength got enhanced up to 1.376 MPa. Similar kind of behavior is observed when CB-HA scaffolds

are coated with PVA and get compressive strength value up to 0.95 MPa. Both of the polymers, PVA and PCL, used are regarded as versatile materials for different kind of potential biomedical applications.

3.5 Porosity

The porosity of the samples measured is given below in Table 2.

Sample Names	Porosity %
CB	73.4
PVA coated CB	69.9
CB-HA	76.1
PVA coated CB-HA	73.6
PCL coated CB-HA	74.1

Table 2: Porosity %age of the samples

The variation in the porosity in the samples, although small, follows a logical trend. Raw CB is 73.4% porous and its porosity decreased after the coating of PVA due to the layer of polymer. The porosity was 76.1% (maximum) when CB is hydrothermally treated due the burning of organic materials present inside CB that's also lead to decrease (lowest) in the mechanical strength as discussed in the section 4.4. When CB-HA is coated with polymers, PVA and PCL, the porosity is decreased to 73.6% and 74.1% respectively which is due to the thin layer of polymers. That's why their mechanical strength values are little higher than CB-HA.

3.6 Cell Viability

MTT assay has been employed to inspect the viability of the rMSC grown with commercial HA, cuttlefish derived HA and cuttlefish derived HA coated with PVA scaffolds. MSC are capable of differentiating into multiple cell lineages such as bone, cartilage, tendon, muscle, and adipose²³. Our results demonstrate no significant difference in % viability of cells grown with the scaffolds compared with TCP control (Tissue Culture Plate) (Fig 5.). These results further suggest that none of the scaffolds included in study alter the proliferation capacity and viability of rMSC.

3.7 Cell Attachment

SEM analysis were carried out to investigate the rMSC attachment on the pure HA, cuttlefish bone derived HA and cuttlefish bone derived HA coated with PVA scaffolds. It is observed that the cells adhere well to surface of scaffolds (Fig 6.). Altogether the SEM data suggest that rMSC can attach and spread on all the scaffolds in this study.

4 Conclusion

In this study we have demonstrated successful transformation of CB, collected from Pakistan sea shores near Karachi, into HA preserving the natural well-interconnected highly porous structure containing parallel pillars. The phase conversion of aragonite (CB) into calcium phosphate (HA) is confirmed by FT-IR and XRD analysis. Subsequently, the scaffolds were coated with PCL and PVA. The uniformity of coating was confirmed by SEM analysis. Coated and non-coated scaffolds were immersed in the SBF solution. UTM analysis revealed that coated scaffolds retain its mechanical

integrity with the formation of apatite layer on it while non-coated scaffolds disintegrate in the solution. The compressive strength increased substantially when CB-HA scaffolds were coated with PVA and PCL. With PCL coating its compressive strength got enhanced up to 1.376 MPa.

In vitro biological evaluation of these materials was carried out using rMSC. Our results showed the cell attachment on these scaffolds and furthermore these materials don't exhibit cytotoxic effect. Bone differentiation assay will be further performed to evaluate the potential role of these materials in bone tissue engineering. .

Acknowledgement

The authors are grateful to HEC, Govt. of Pakistan, for providing funds under NRPU project No. 1835 and HEC Mega PC-1 and MoST P-1 of Government of Pakistan.

References

1. J. C. B. S.F. Hulbert, L.L. Hench, J. Wilson, G. Heimke, *High Tech Ceramics A*, 1987, 189-213.
2. P. Sepulveda, J. G. P. Binner, S. O. Rogero, O. Z. Higa and J. C. Bressiani, *Journal of Biomedical Materials Research*, 2000, **50**, 27-34.
3. Z. Y. Wu, R. G. Hill and J. R. Jones, *Bioceramics Development and Applications*, **1**.
4. B. C. R.Z. Le Geros ed. by P.W. Brown, *CRC Press, Boca Raton*, 1994, 3.
5. D. Green, D. Walsh, S. Mann and R. Oreffo, *Bone*, 2002, **30**, 810-815.
6. J. Hu, J. J. Russell, B. Ben-Nissan and R. Vago, *Journal of Materials Science Letters*, 2001, **20**, 85-87.
7. Y. Xu, D. Wang, L. Yang and H. Tang, *Materials Characterization*, 2001, **47**, 83-87.
8. K. S. Vecchio, X. Zhang, J. B. Massie, M. Wang and C. W. Kim, *Acta Biomaterialia*, 2007, **3**, 910-918.
9. H. Ivankovic, G. G. Ferrer, E. Tkalcec, S. Orlic and M. Ivankovic, *J Mater Sci: Mater Med*, 2009, **20**, 1039-1046.
10. D. M. Roy and S. K. Linnehan, *Nature*, 1974, **247**, 220-222.
11. M. Sivakumar, T. S. S. Kumar, K. L. Shantha and K. P. Rao, *Biomaterials*, 1996, **17**, 1709-1714.
12. J. H. G. Rocha, A. F. Lemos, S. Agathopoulos, P. Valério, S. Kannan, F. N. Oktar and J. M. F. Ferreira, *Bone*, 2005, **37**, 850-857.
13. D. Milovac, T. C. Gamboa-Martínez, M. Ivankovic, G. G. Ferrer and H. Ivankovic, *Materials Science and Engineering: C*, 2014, **42**, 264-272.
14. B. S. Kim, J. S. Kim, H. M. Sung, H. K. You and J. Lee, *Journal of Biomedical Materials Research Part A*, 2012, **100**, 1673-1679.
15. H. Mehboob, M. Awais, H. Khalid, S. A. Siddiqi and I. Rehman, *Biomedical Engineering: Applications, Basis and Communications*, 2014, **26**, 1450073.
16. K. J. Kim HW, Kim HE, *Biomaterials*, 2004, **25**, 1279-1287.
17. C. Agrawal and R. B. Ray, *Journal of Biomedical Materials Research*, 2001, **55**, 141-150.
18. S. Orlić, H. Ivanković and E. Tkalčec, *University of Zagreb, Faculty of*, 2005.

19. B. S. Kim, H. J. Kang and J. Lee, *J Biomed Mater Res B Appl Biomater*, 2013, **101**, 1302-1309.
20. T. Kokubo and H. Takadama, *Biomaterials*, 2006, **27**, 2907-2915.
21. Y. Zhang and M. Zhang, *Journal of Biomedical Materials Research*, 2001, **55**, 304-312.
22. X. Li, Y. Zhang and G. Qi, *Cytotechnology*, 2013, **65**, 323-334.
23. E. Battistella, S. Mele, S. Pietronave, I. Foltran, G. Lesci, E. Foresti, N. Roveri and L. Rimondini, 2010.
24. S. Perveen, A. Al-Taweel, G. Fawzy, A. El-Shafae, A. Khan and P. Proksch, *Pharmacognosy Magazine*, 2015, **11**, 1-5.
25. D. F. G errard Eddy Jai Poinern, *American Journal of Materials Science*, 2013, **5**, 130-135.
26. J. Rocha, A. Lemos, S. Agathopoulos, P. Val erio, S. Kannan, F. Oktar and J. Ferreira, *Bone*, 2005, **37**, 850-857.
27. B. Fowler, *Inorganic Chemistry*, 1974, **13**, 194-207.
28. A. C. Joris SJ, *J Phys Chem*, 1971, **75**, 3172-3178.
29. A. A. Chaudhry, J. C. Knowles, I. Rehman and J. A. Darr, *Journal of Biomaterials Applications*, 2013, **28**, 448-461.
30. N. Chickerur, M. Tung and W. Brown, *Calcified Tissue International*, 1980, **32**, 55-62.
31. A. Polini, D. Pisignano, M. Parodi, R. Quarto and S. Scaglione, *PloS one*, 2011, **6**, e26211.
32. S. Yuan, G. Xiong, X. Wang, S. Zhang and C. Choong, *Journal of Materials Chemistry*, 2012, **22**, 13039-13049.
33. J. H. G. Rocha, A. F. Lemos, S. Agathopoulos, P. Val erio, S. Kannan, F. N. Oktar and J. M. F. Ferreira, *Bone*, **37**, 850-857.

Figure Captions

Figure 1: XRD pattern of (a) HA, (b) cuttlefish bone

Figure 2: FTIR spectra (a) CB (b) HA-CB (c) PVA coated HA-CB (d) PCL coated HA-CB (e) SBF studies HA- CB (f) SBF studied on PCL coated HA-CB (g) PVA coated CB

Figure 3: SEM micrograph of (a) Raw Cuttlebone, CB, (b) PVA coated Cuttlebone (c) PCL Coated HA- CB scaffolds (d) SBF study of raw cuttlebone (e) SBF study of PCL coated HA-CB scaffolds

Figure 4: Graphical representation of compressive strength by UTM analysis

Figure 5: % Viability of rat mesenchymal stem cells (rMSC) seeded in TCP (Tissue Culture Plate) control, with hydroxyapatite (HA) scaffolds, cuttlefish bone derived HA and cuttlefish bone derived HA coated with poly vinyl alcohol (PVA) determined by MTT assay after 7 days of culturing. Bars represent mean cell viability normalized to control cells and error bars depict the standard deviation of three independent experiments (n = 3)

Figure 6: SEM micrographs of A) HA, B) cuttlefish bone derived HA, and C) cuttlefish bone derived HA coated with PVA scaffolds seeded with rMSC after 7 days of culturing. The images B) and C) depict single cell attachment

Figures

Figure 1

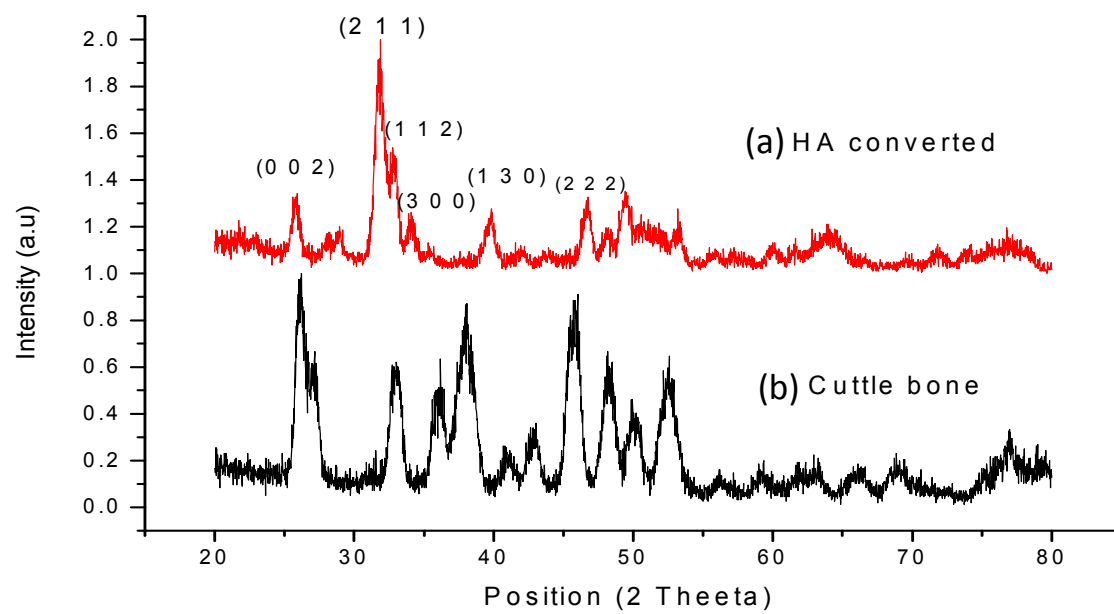


Figure 2

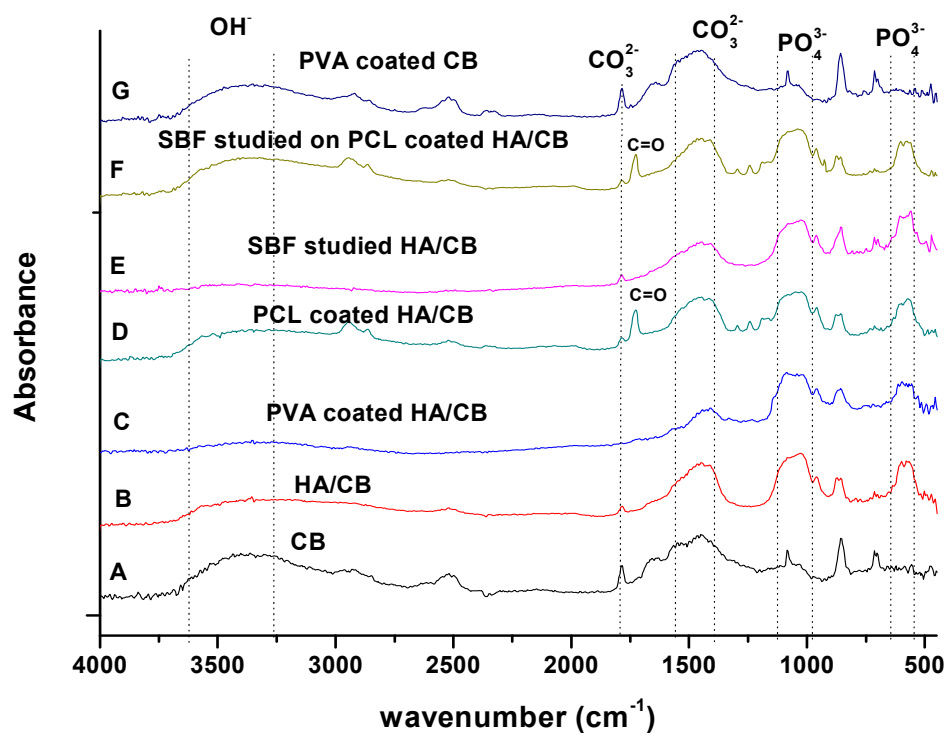


Figure 3

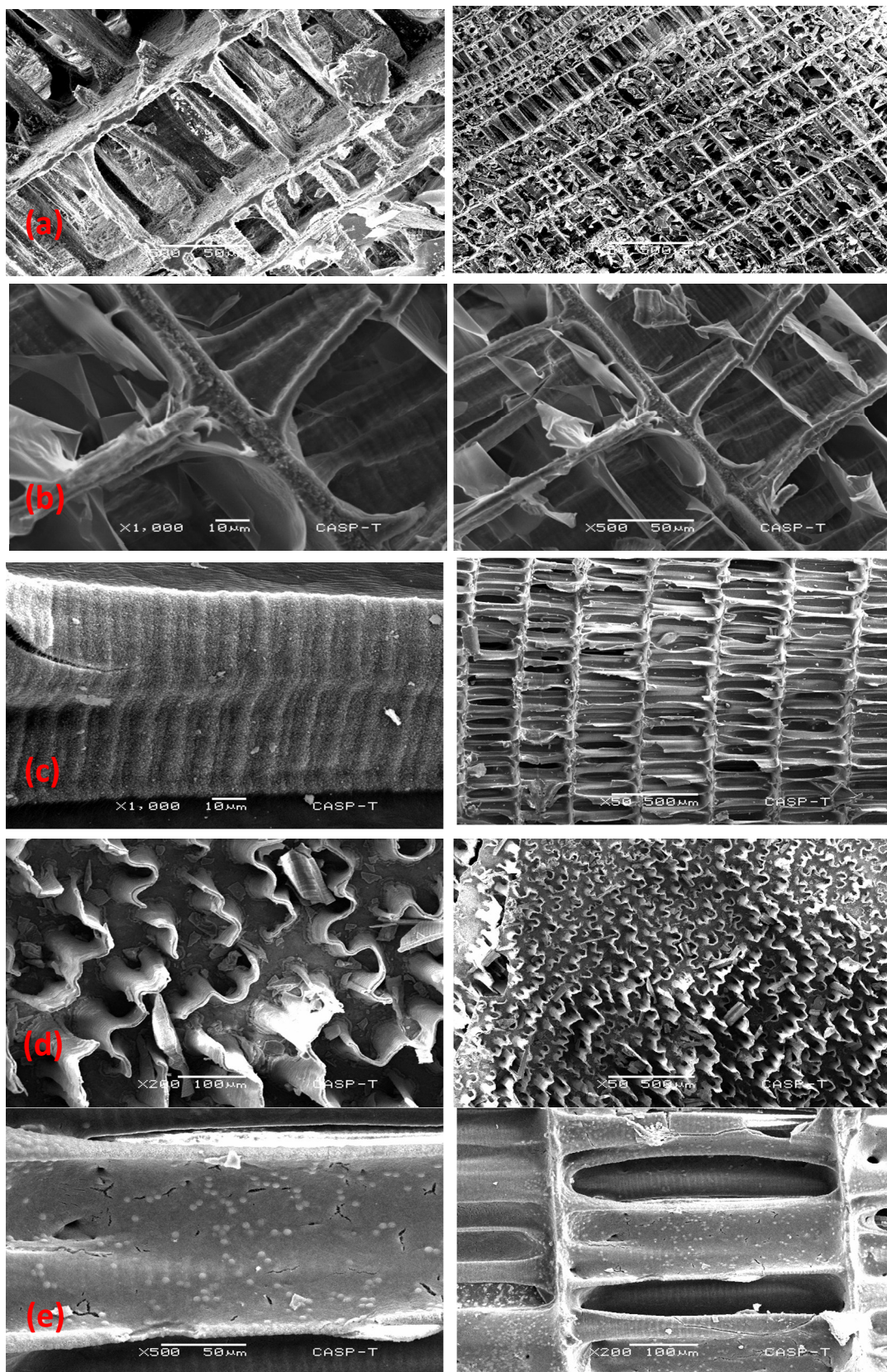


Figure 4

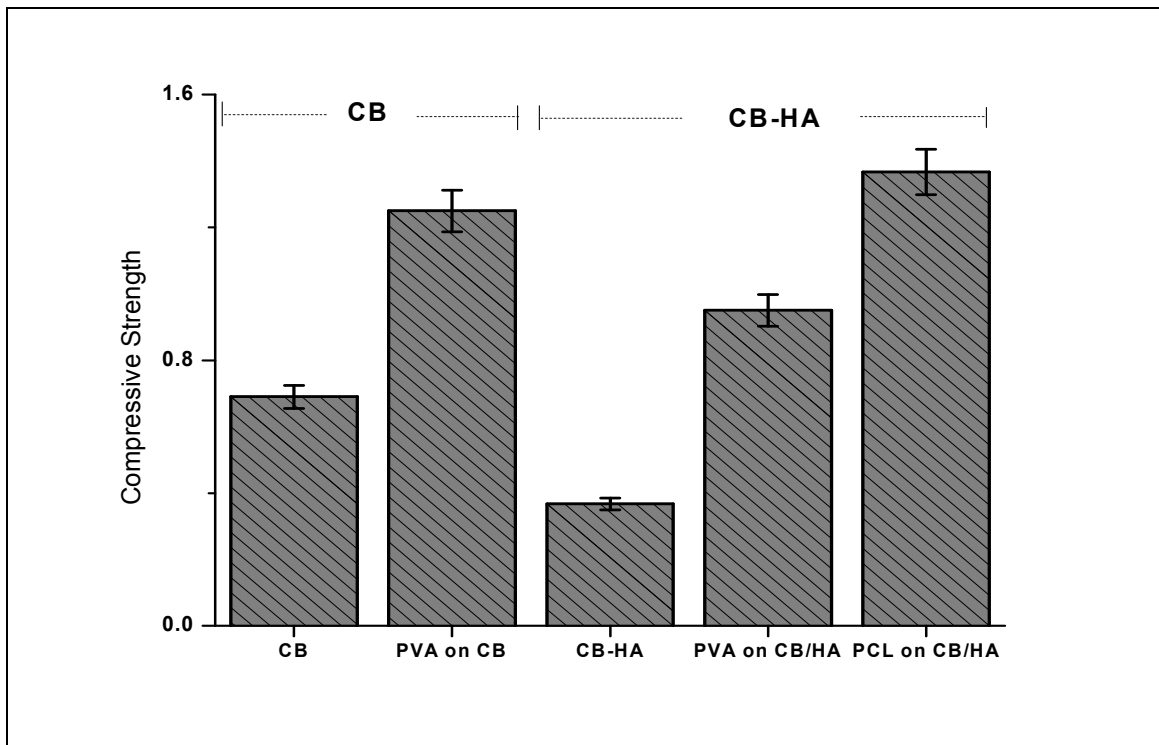


Figure 5

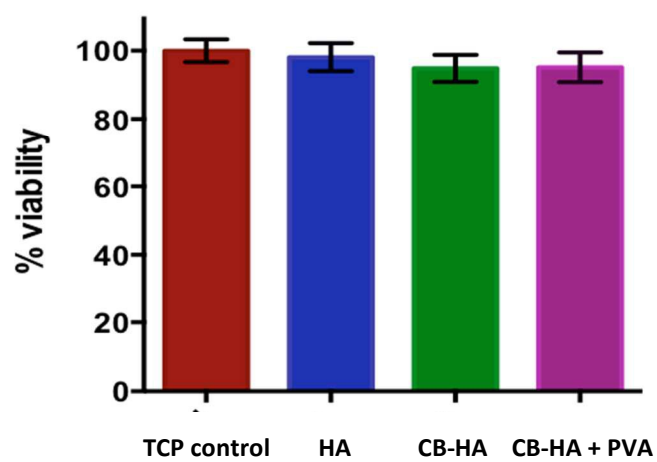


Figure 6

